Astron. Astrophys. 342, 655–664 (1999)

ASTRONOMY
AND
ASTROPHYSICS

Star formation and the interstellar medium in low surface brightness galaxies

III. Why they are blue, thin and poor in molecular gas

Jeroen P.E. Gerritsen and W.J.G. de Blok⋆

Kapteyn Astronomical Institute, Postbus 800, 9700 AV Groningen, The Netherlands

Received 17 July 1997 / Accepted 9 November 1998

Abstract. We present N-body simulations of Low Surface Brightness (LSB) galaxies and their Interstellar Medium to investigate the cause for their low star formation rates (SFR).

Due to their massive halos, stellar disks of LSB galaxies are very stable and thin. Lack of dust makes the projected edge-on surface brightness of LSB galaxies comparable to the projected edge-on surface brightness of dust-rich High Surface Brightness (HSB) galaxies of similar size.

We show that the low surface densities found in LSB galaxies are by themselves not enough to explain the slow evolution of LSB galaxies. A low metal content of the gas is essential. As a consequence the gas cools inefficiently, resulting in an almost negligible cold gas fraction. We show that LSB galaxies must have molecular gas fractions of less than 5 percent.

Our best model has a SFR which is on average low but fluctuates strongly. This causes the large spread in colors of LSB galaxies. From a distribution of birthrate parameters we conclude that the presently-known and modeled gas-rich blue LSB galaxies constitute the majority of the total population of gas-rich LSB disk galaxies. We deduce the existence of an additional red, quiescent and gas-rich population which constitutes less than 20 percent of the total population. This does not rule out the existence of a large number of gas-poor LSB galaxies. These must however have had an evolutionary history dramatically different from that of the gas-rich galaxies.

Key words: methods: numerical – hydrodynamics – galaxies: spiral – galaxies: evolution

1. Introduction

Deep surveys of the night-sky have uncovered a large population of disk galaxies with properties quite different from those of the extensively studied "normal" high surface brightness (HSB) galaxies. These so-called Low Surface Brightness (LSB) galaxies have, as their name already implies, surface brightnesses much lower than what was until quite recently assumed to be representative for disk galaxies (Freeman 1970).

The LSB galaxies we will be discussing are generally dominated by an exponential disk, with scale lengths of a few kpc. Morphologically they form an extension of the Hubble sequence towards very late-type galaxies. Observations suggest that LSB galaxies are unevolved galaxies, as shown by e.g. the subsolar metallicities (McGaugh 1994) and the colors (McGaugh & Bothun 1994; de Blok et al. 1995; van den Hoek et al. 1997).

The evolutionary rate of a galaxy may in fact be reflected in its surface brightness. For example, the gas fraction ($M_{\rm gas}/M_{\rm gas+stars}$) increases systematically with surface brightness, from a few percent for early type spirals to much higher values approaching unity for late type LSB galaxies (de Blok & McGaugh 1996). In many LSB galaxies the gas mass exceeds the stellar mass (even for such extreme assumptions as maximum disk).

It is still unclear what the physical driver is for the difference between HSB and LSB galaxies. Investigations of their dynamics, using H I observations (de Blok et al. 1996), suggest that LSB galaxies are low-density galaxies (de Blok & McGaugh 1996). This is one of the favored explanations for the low evolution rate of LSB galaxies (see e.g. van der Hulst et al. 1987), as this implies a large dynamical time-scale. Environment may also play a role. Tidal interactions with other galaxies increase star formation rates. This may not happen in LSB galaxies which are found to be isolated (Mo et al. 1994). In LSB galaxies a few star forming regions are usually found. These are distributed randomly over the galaxies and do not trace the spiral arms.

The main purpose of this paper is to investigate whether the low density alone can explain the properties of LSB galaxies. We use 3D numerical simulations to address this problem. The dynamical simulations include both stars and gas and incorporate a parameterized description of star formation, including feedback on the gas.

The prescription of star formation in numerical simulations is not straightforward, given the limited resolution of the models and the fragmentary knowledge about the physics governing star formation on kpc scales. In the literature various different star

⋆ *Present address:* School of Physics, University of Melbourne, Parkville, VIC 3052, Australia

formation algorithms can be found. For instance, Friedli & Benz (1995) use a criterion based on the Toomre stability parameter Q (Toomre 1964) to study star formation in barred systems; Mihos & Hernquist (1994a,b, 1996) adopt a Schmidt law based on the gas density [star formation rate (SFR) $\propto \rho^{1.5}$] to study mergers of galaxies; others require gas to be in a convergent and Jeans unstable flow to form stars (Katz 1992; Katz et al. 1996; Navarro & White 1993; Steinmetz 1996).

We employ the method of Gerritsen & Icke (1997, 1998), which uses a Jeans criterion to define star forming regions, coupled with an estimate of the cloud collapse time. In these simulations gas is treated fully radiative with allowed temperatures between 10 K and 10^7 K; cooling is described by standard cooling functions, heating is assumed to be provided by far-ultraviolet (FUV) radiation and mechanical heating from stars. In this way the simulated interstellar medium (ISM) mimics a multi-phase ISM (Field et al. 1969; McKee & Ostriker 1977). This is an improvement over other simulations which try to create a multi-phase ISM but do not allow radiative cooling below 10^4 K (e.g. Hernquist 1989; Katz et al. 1996). The multi-phase ISM allows us to restrict ourselves to considering only relatively cold ($T < 10^3$ K) regions as the sites for star formation.

Here we apply this method to study the ISM and star forming properties of LSB galaxies, and our results will be valid under the assumption that the physical processes governing star formation are the same for HSB and LSB galaxies. We test whether a low mass-density is sufficient to explain the properties of LSB galaxies by discussing two different models of a specific LSB galaxy: the first model has the cooling properties of a solar abundance ISM, while in the second model the cooling efficiency is lowered, thus mimicking a metal-poor ISM.

The structure of the paper is as follows. In Sect. 2 we describe the numerical techniques. The construction of a model LSB galaxy is presented in Sect. 3. This galaxy model is evolved for a few Gyr, using two different prescriptions for the cooling properties of the gas (Sect. 4). The implications of the simulations are discussed in Sect. 5. We conclude this paper with a summary in Sect. 6.

2. Numerical technique

We model the evolution of galaxies using a hybrid *N*-body/hydrodynamics code (TREESPH; Hernquist & Katz 1989). An extensive description is given in Gerritsen & Icke (1997, 1998). A tree algorithm (Barnes & Hut 1986; Hernquist 1987) determines the gravitational forces on the collision-less and gaseous components of the galaxies. The hydrodynamic properties of the gas are modeled using smoothed particle hydrodynamics (SPH) (see Lucy 1977; Gingold & Monaghan 1977). The gas evolves according to hydrodynamic conservation laws, including an artificial viscosity for an accurate treatment of shocks. Each particle is assigned an individual smoothing length, h, which determines the local resolution and an individual time step. Estimates of the gas properties are found by smoothing over 32 neighbors within $2h$. We adopt an equation of state for an ideal gas.

We allow radiative cooling of the gas according to the cooling function for a standard hydrogen gas mix with a helium mass fraction of 0.25 (Dalgarno & McCray 1972). Radiative heating is modeled as photo-electric heating of small grains and PAHs by the FUV field (Wolfire et al. 1995), produced by the stellar distribution.

All our simulations are advanced in time steps of 3×10^6 yr for star particles, while the time steps for SPH particles can be 8 times shorter (3.8×10^5 yr). The gravitational softening length is 150 pc. A tolerance parameter $\theta = 0.6$ is used for the force calculation, which includes quadrupole moments.

2.1. Star formation and feedback

Gerritsen & Icke (1997, 1998) extensively describe the recipe for transforming gas into stars and the method for supplying feedback onto the gas. The recipe works well for normal HSB galaxies, with the energy budget of the ISM as prime driver for the star formation. The simulations allow for a multi-phase ISM with temperature between $10 < T < 10^7$ K. This allows us to consider cold $T < 10^3$ K regions as places for star formation (Giant Molecular Clouds in real life). Below we summarize the important ingredients of the method.

From our SPH particle distribution we select conglomerates where the Jeans mass is below the mass of a typical Giant Molecular Cloud. In the simulations performed here we use $M_c = 10^6\ M_\odot$ for this aggregate mass (the method is not very sensitive to the exact value for this mass). The Jeans mass depends on the local gas properties and is calculated from the SPH estimates of the density ρ and sound speed s,

$$M_J = \frac{1}{6}\pi\rho\left(\frac{\pi s^2}{G\rho}\right)^{\frac{3}{2}}, \tag{1}$$

with G the constant of gravity. During the simulations the maximum number density achieved is of the order 1 cm^{-3}. It follows that only regions below 10^3 K are unstable and may form stars.

We follow unstable regions during their dynamical and thermal evolution and if an SPH particle resides in such a region longer than the collapse time,

$$t_u > t_c = \frac{1}{\sqrt{4\pi G\rho}}, \tag{2}$$

half of its mass is converted into a star particle. Experiments with a different number of particles and different star formation efficiencies show no dependence on these parameters, as already shown in Gerritse & Icke (1997).

Important for our calculations is that we consider star particles as stellar clusters with an age. Thus for each individual star particle we can attribute quantities like the SN-rate, the mass loss, and the FUV-flux, according to its age. We use the spectral synthesis models of Bruzual & Charlot (1993) to determine these quantities, where we adopt a Salpeter Initial Mass Function (IMF) with slope 1.35 and with lower and upper mass limits of $0.1\ M_\odot$ and $125\ M_\odot$ respectively.

The radiative heating for a gas particle is calculated by adding the FUV-flux contributions from all stars, which is done

Table 1. Parameters for F563-1 (H_0 = 75 km s^{-1} Mpc^{-1}).

L_B	$1.35 \times 10^9\ L_\odot$	
h_*	2.8 kpc	center ($R < 5$ kpc)
h_*	5.0 kpc	outside ($R > 5$ kpc)
SFR	0.05 $M_\odot$/yr	
$M_{\rm H\,I}$	$2.75 \times 10^9\ M_\odot$	
$v_{\rm max}$	113 km s^{-1}	
$\rho_0^{\rm halo}$	0.0751 $M_\odot$/pc^3	
$R_c^{\rm halo}$	1.776 kpc	

together with the force calculation. The mechanical luminosity from a star particle is determined by both the SN-rate and the mass loss rate. We assume that each SN injects 10^{51} ergs of energy and that the energy injected by stellar winds is $E_w = \frac{1}{2}\Delta m_* v_\infty^2$, with v_∞ the wind terminal velocity and Δm_* the stellar mass loss. For massive stars v_∞ depends critically on the stellar mass, luminosity, effective temperature, and metallicity (e.g. Leitherer et al. 1992; Lamers & Leitherer 1993). For simplicity we adopt $v_\infty = 2000$ km s^{-1}. After 3.3×10^7 yr the last $8\ M_\odot$ stars explode and no more mechanical energy is supplied to the gas. Thus we return mechanical energy from massive stars into the ISM, and ignore the mechanical energy from low mass stars.

In the simulations the parent SPH particle is the carrier of the mechanical energy from the new star particle. This SPH particle ("SN particle") mimics a hot bubble interior. Radiative cooling is temporarily switched off (the resolution does not allow the creation of a low-density, hot bubble), the temperature of the SN particle is set to the mechanical energy density (of a few 10^6 K), and the particle evolves adiabatically. The first 10^7 yr, the position and velocity of the SN particle are equal to the position and velocity of the associated star particle. Afterwards, the SN particle evolves freely. After 3×10^7 yr radiative cooling is switched on again, and the particle behaves like an ordinary SPH particle.

3. Modeling an LSB galaxy

There are many ways to construct model galaxies. For our purpose we prefer to build a galaxy model after an existing galaxy with well-determined properties. Here we choose LSB galaxy F563-1; this galaxy is a late-type LSB galaxy, representative of the field LSB galaxies found in the survey by Schombert et al. (1992). The optical properties of this galaxy are described in de Blok et al. (1995); measurements of metallicities in H II regions are described in de Blok & van der Hulst (1998a); a neutral hydrogen map and rotation curve are given in de Blok et al. (1996). Parameters such as stellar velocity dispersion, which cannot be measured directly, are set in comparison with values measured locally in the Galaxy. The current star formation rate as deduced from Hα imaging is taken from van den Hoek et al. (1997). For convenience these data are summarized in Table 1.

The most difficult problem we face in constructing a model is converting the measured luminosity to a stellar disk mass. This is one of the most persistent problems in analyzing the dynamics of galaxies, and, unfortunately, the present observations do not provide a unique answer for this stellar disk mass-to-light ratio $(M/L_B)_*$. Rather than using the so-called "maximum disk" value $(M/L_B)_* = 9$, which is an upper limit to the possible values of $(M/L_B)_*$, we adopt a value based on colors and velocity dispersions of $(M/L_B)_* = 1.75$. An extensive motivation for this choice is given by de Blok & McGaugh (1997). The implications of choosing a different value of $(M/L_B)_*$ for the evolution of the stellar disk will be discussed in Sect. 3.2.

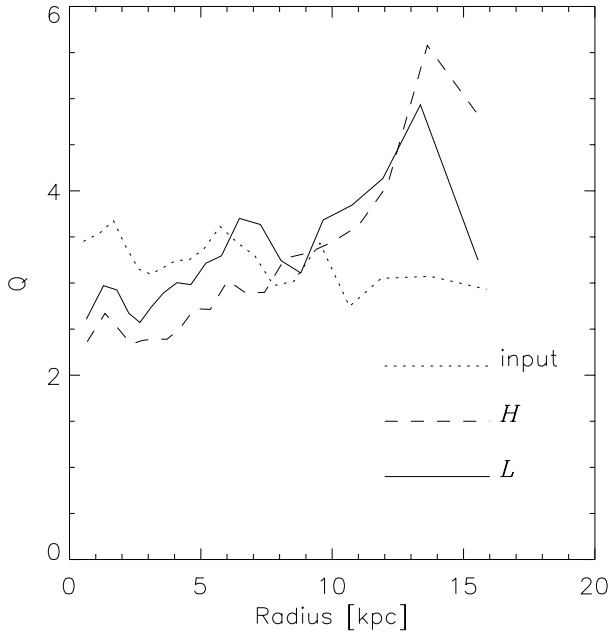

Fig. 1. The stability parameter Q versus radius. The dotted line shows the Q-value upon initialization of the galaxy model. The solid line denotes simulation L, the dashed line simulation H. Both simulation yield approximately the same stability for the stellar disk

3.1. The model

The stellar disk particles are distributed radially according to the (measured) surface density profile. We adopt a vertical distribution of the form sech$^2(z/z_*)$ (e.g. van der Kruit & Searle 1982), with a constant vertical scale height $z_* = 0.5$ kpc The disk is truncated at 25 kpc. The luminosity yields a total stellar mass of $M_* = 2.36 \times 10^9\ M_\odot$. The velocity dispersion of the stars is fixed via the relation

$$\sigma_z = \sqrt{\pi G z_* \Sigma_*}, \tag{3}$$

where Σ_* is the stellar surface density. This implies a stability parameter $3 < Q < 3.5$ throughout for the disk (dotted line in Fig. 1).

Particle velocities are assigned according to the (gas) rotation curve corrected for asymmetric drift. Dispersions in R, z, θ directions are drawn from Gaussian distributions with dispersions of $\sigma_R, \sigma_z, \sigma_\theta$ respectively, using the relations valid for the solar neighborhood

$$\sigma_z = 0.6\sigma_R, \;\; \sigma_\theta = \frac{\kappa}{2\omega}\sigma_R, \tag{4}$$

with ω and κ the orbital and epicyclic frequencies respectively.

The gas surface density distribution is modeled after the H I distribution. The total gas mass is $M_g = 3.85 \times 10^9\ M_\odot$ (this is the total H I mass multiplied by 1.4 to include He); the surface density decreases almost linearly with radius out to 33 kpc. The vertical distribution is assumed to decline exponentially. The scale height z_g of the gas layer can be calculated using

$$\sigma_g^2 = 2\pi G(\Sigma_g + \Sigma_*)\frac{z_g^2}{\frac{1}{2}z_* + z_g}, \tag{5}$$

(Dopita & Ryder 1994) where $\sigma_g = 3\,\mathrm{km\,s^{-1}}$ is the (adopted) gas velocity dispersion. The gas particles are assigned velocities according to the rotation curve, with isotropic dispersion σ_g.

The halo is included in the calculations as a rigid potential. This is justified since the galaxy model evolves in isolation. We will thus also ignore any contraction of the halo under the influence of the disk potential. We do not expect this effect to be important anyway as the mass of the disk (assuming $(M/L_B)_* = 1.75$) is only 4 per cent of the measured halo mass (de Blok & McGaugh 1997). As advantages we do not have to make assumptions about halo particle orbits, and we do not have to spend time in calculating the force of the halo particles on the galaxy. We assign an isothermal density distribution to the halo,

$$\rho_h = \frac{\rho_0}{1 + (r/R_c)^2}, \tag{6}$$

with central volume density $\rho_0 = 0.0751 M_\odot/\mathrm{pc}^3$ and core radius $R_c = 1.776$ kpc. These are the values derived from a rotation curve decomposition assuming $(M/L_B)_* = 1.75$. This will correctly put the maximum rotation velocity at 113 km s^{-1}.

For the simulations we use 40,000 SPH particles and 80,000 star particles initially. This corresponds to an SPH particle mass of $9.6 \times 10^4\ M_\odot$ and a star particle mass of $3.0 \times 10^4\ M_\odot$.

3.2. Implications of $(M/L_B)_*$ for star formation history

We can show that a maximum disk value for $(M/L_B)_*$ is not a plausible option for our modeling exercise, and that in fact the "most likely" value we use in constructing models may still overestimate the true value of $(M/L_B)_*$, making the stellar disk a really insignificant component of the whole galaxy system.

The star formation history of galaxies is commonly parameterized by an exponential function:

$$\mathrm{SFR} = -\dot{M}_g = M_g/\tau_* \tag{7}$$

where τ_* is the star formation time scale (e.g. Guiderdoni & Rocca-Volmerange 1987 and Charlot & Bruzual 1991). This ignores any gas locked up in long-lived stars, but this effect will not be important in LSB galaxies due to their large gas-fractions. A small value for τ_* means that star formation proceeds rapidly, while a large τ_* indicates that star formation proceeds very slowly.

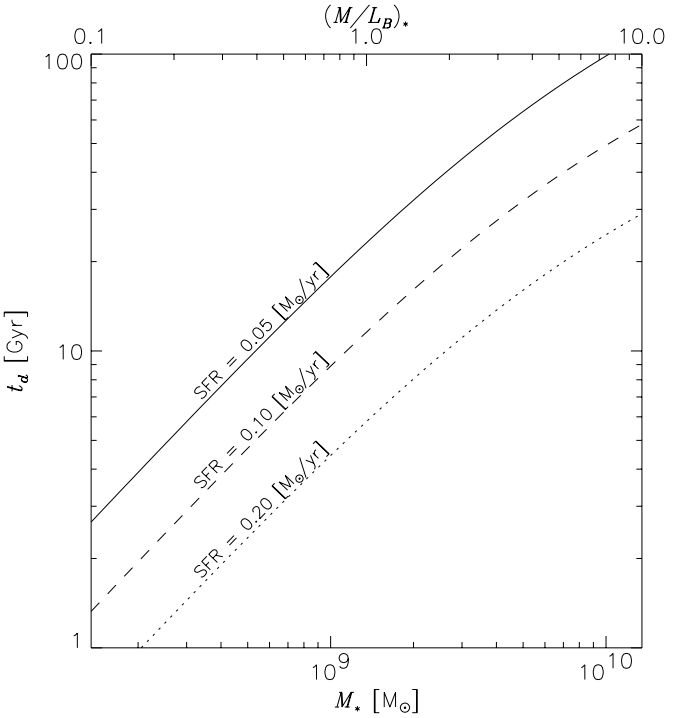

Fig. 2. Relation between galaxy age, t_d (vertical axis), and stellar mass, M_* (horizontal axis), according to Eqs. 7 and 8. The different lines are solutions to these equations for various values of the current SFR, where the measured value is $0.05\ M_\odot$/yr. The top axis shows the $(M/L_B)_*$ ratio corresponding to the stellar mass. The input model assumes $(M/L_B)_* = 1.75$, the maximum disk model has $(M/L_B)_* = 9$, which yields a very high age for the galaxy

For HSB galaxies the star formation time scale is normally a few Gyr (Kennicutt et al. 1994). For F563-1 the measured current SFR as derived from Hα imaging is approximately $0.05\ M_\odot$/yr; this yields a star formation time scale of 77 Gyr. Thus star formation in this disk proceeds much slower than in HSB galaxies.

Since we know the stellar and gas mass, and hence the total disk mass $M_t = M_* + M_g$ of the galaxy, we can use the exponential parameterization and the known SFR to compute the "age" t_d of the disk (i.e. the time elapsed since star formation started):

$$M_* = -\int_0^{t_d} \dot{M}_g dt = M_t\left(1 - \mathrm{e}^{-t_d/\tau_*}\right). \tag{8}$$

For the adopted stellar mass of F563-1 Eq. 8 yields an age for the galaxy of 37 Gyr, much larger than the age of the universe.

If the exponentially declining SFR describes the star formation history adequately and the galaxy is not in a state of unusually low star formation activity (note that the blue colors for these LSB galaxies suggest a relatively *high* current star formation activity), then the old implied age of the disk could mean that the mass of the disk should in reality be even less.

We show this in Fig. 2 where we present a few solutions for Eqs. 7 and 8 for various values of the SFR. If we adopt $0.05\ M_\odot$/yr as the true SFR then $(M/L_B)_* \approx 0.6$ if the

galaxy is 15 Gyr old. Higher values for $(M/L_B)_*$ would make the galaxy older than the universe. A maximum disk solution (van Albada & Sancisi 1986) for the stellar mass-to-light ratio yields $(M/L_B)_* = 9$, which leads to an age of 110 Gyr. A current SFR of order $0.4\ M_\odot$/yr is needed to reconcile the maximum disk with the exponentially declining SFR model, which implies that the measurements underestimate the true SFR by an order of magnitude. Thus seems highly unlikely (it would give LSB galaxies SFRs comparable to those of actively star forming late type galaxies), and therefore we reject the maximum disk as an acceptable solution for the stellar disk mass.

The adopted $(M/L_B)_* = 1.75$ which we use in the galaxy model is only consistent with the age of the universe if the true SFR is of order $0.10\ M_\odot$/yr, otherwise the stellar mass is probably overestimated. However if the stellar disk is indeed less massive than our galaxy model, then any conclusions concerning the disk stability and thickness of the disk will be even stronger.

It might be argued that the exponential star formation history is not the right choice for this type of galaxy, and that other functional forms of star formation history, in combination with the measurements, will yield reasonable ages. This is not true, as any other (reasonable) star formation history will result in even larger ages for the disk. Taking for example another extreme functionality – a constant SFR of 0.05 $M_\odot$/yr – yields an age $t_d = 47$ Gyr. The only way to get a reasonable age, given the measured luminosity and assumed $(M/L_B)_*$, is to assume that the current SFR in F563-1 (and LSB galaxies in general) has been underestimated, which is unlikely. We refer to McGaugh & de Blok (1997) for an extensive discussion on the various functionalities of the star formation history.

We therefore conclude that the disk of F563-1 must have a small stellar mass-to-light ratio.

4. Evolution

In this section we demonstrate that the low density as found in LSB galaxies, by itself is not sufficient to reproduce the low observed SFRs of LSB galaxies. *Low metallicity gas is required to explain the properties of LSB galaxies.*

To show this we construct two model galaxies using the structural parameters of F563-1. Model H represents an LSB galaxy with a solar metallicity gas. Although we use the structural parameters relevant for F563-1, the model is in effect a model HSB galaxy, which is "stretched out" to give the low (surface) densities found in LSB galaxies. This model therefore tests the low-density hypothesis.

The other model, L, has the same structural parameters as H, but in addition we lowered the cooling efficiency of the gas below 10^4 K by a factor of seven. Cooling below 10^4 K is dominated by metals, so lowering the efficiency is equivalent to lowering the metallicity by an equal amount. Model L thus most closely approximates what is currently known observationally about LSB galaxies. In summary we adopt the cooling function of a solar abundance gas in model H. This cooling function is later changed in model L to simulate the effects of low metallicity.

We assume that the physics regulating the star formation is the same for LSB and HSB galaxies, and therefore use the star formation recipe described in Sect. 2 and applied to HSB galaxies in Gerritsen & Icke (1997, 1998). After initialization we let the two model galaxies evolve for 2.3 Gyr. The models rapidly settled into equilibrium, any longer time interval would have produced identical results.

In this section we first discuss the evolution of the stellar disk. The stellar disk evolves rather independently from the gas disk and star formation. Hence we effectively explore the consequences of the disk/halo decomposition, notably on the stability and thickness of the stellar disk. Second, we discuss the evolution of the SFR with time for both simulations. For a physical interpretation of the difference in SFRs we present phase diagrams of the ISM in both simulations.

4.1. Stellar disk

Fig. 1 shows the stability parameter Q for the stellar disk at $t = 2$ Gyr (that is 2 Gyr after the start of the simulation which started at $t = 0$), where Q is defined as

$$Q = \frac{\kappa\sigma_R}{3.36G\Sigma_*}, \tag{9}$$

with κ the epicycle frequency (Toomre 1964). $Q < 1$ denotes a (local) instability, while $Q > 1$ means stability. For both simulations $Q \approx 2.5$ in the center and rises to $Q \approx 5$ in the outer parts of the disk. There is no evolution in the stability. Once the system has settled after the start of the simulation, the radial behavior of Q as shown is reached. The value of course depends on the input parameters, notably the stellar mass, but it is clear that the stellar disks of LSBs are more stable than the stellar disks of HSBs, where Q is of order 2 (Bottema 1993, van der Hulst et al. 1993).

In both simulations the scale height of the stellar disk decreases by approximately a factor of 1.3. The initial scale height corresponded to the scale height of an Sc galaxy (van der Kruit & Searle 1982). The final axial ratio for the galaxy model is about 15. As particle scattering during the simulation tends to increase the thickness of the disk, we conclude that the stellar disks of LSB galaxies are thinner than those of HSB galaxies. We will return to this in more detail in Sect. 5.1.

4.2. Star formation and ISM

Fig. 3 shows the SFR versus time. In model H the SFR settles after a short adjustment at a value of $0.28\ M_\odot$/yr and declines slowly with time. The SFR in model L settles at $0.08\ M_\odot$/yr.

For both simulations the SFR varies on time scales of a few tens of Myr and the amplitude of these variations can exceed $0.1\ M_\odot$/yr. The rapid variability in the SFR is due to the discrete nature of star formation in our simulation. New star particles have a mass of approximately $5 \times 10^4\ M_\odot$ and thus represent (large) stellar clusters. In this way our simulations incorporate the idea that most stars in real galaxies form in stellar clusters.

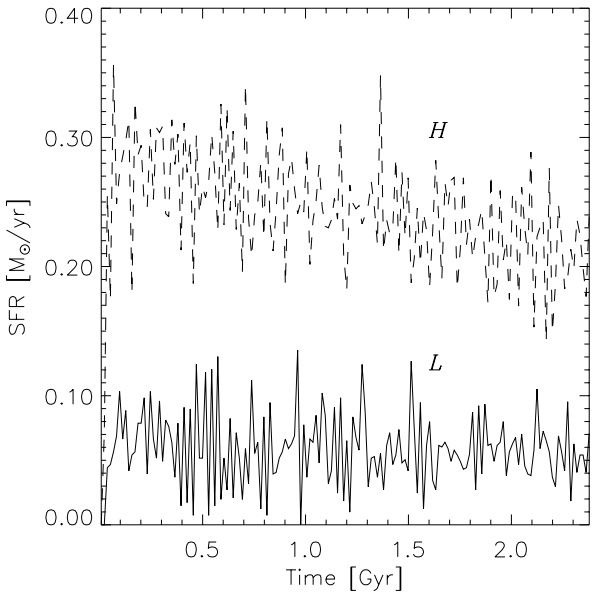

Fig. 3. The evolution of the SFR versus time. The lower line shows the SFR from simulation L, the upper line represents simulation H. Data are averaged over 9 Myr

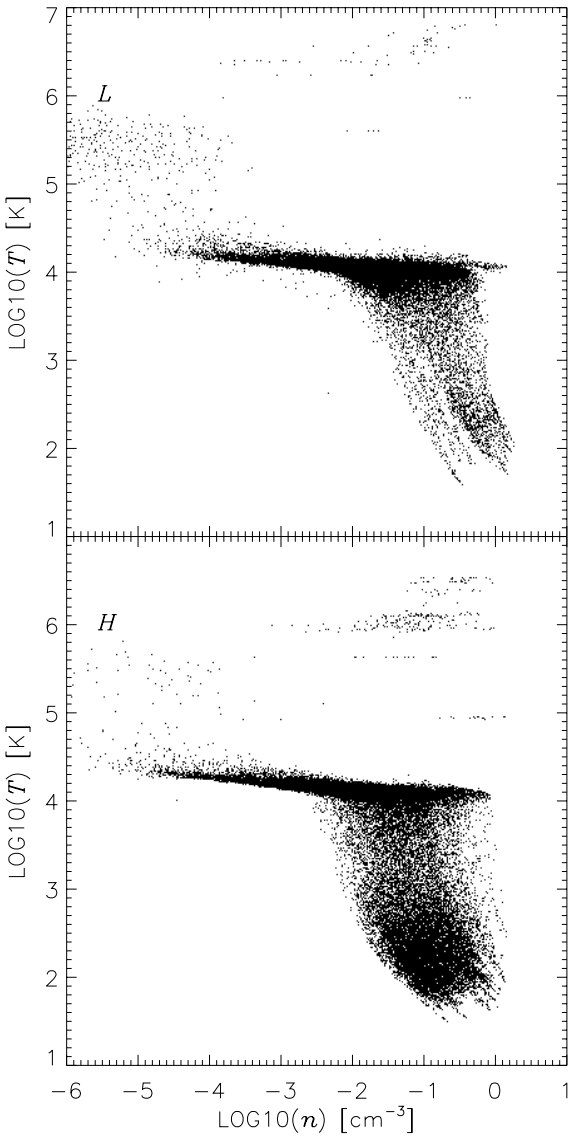

Fig. 4. Phase diagrams (temperature versus number density) for the simulations. *Top panel* shows simulation L, *bottom panel* shows simulation H; each dot represents an SPH particle. The individual particles at the *top* of each diagram are hot SN particles. Simulation H clearly shows a two-phase structure, while in simulation L almost all gas is in the warm ($T \approx 10^4$ K) phase (85%)

For a small number of star forming regions (as in LSB galaxies) this will in real life also lead to a rapidly fluctuating, but on average low SFR.

In simulation L the strength of the star formation peak is large compared to the average SFR. These fluctuations in star formation activity will actually dominate the color of the galaxy, with large fluctuations giving rise to blue colors. The same star formation fluctuations will also be present in HSB galaxies, but due to the higher SFR the large number of fluctuations will give the impression of a high, relatively constant SFR.

We thus find that it is not so much the absolute value of the average SFR which determines the colors, but the contrast of any SF fluctuation with respect to the average SFR. For the LSB galaxies the large contrast leads to blue colors.

In order to understand the behavior of the star formation activity in the simulations we constructed phase diagrams of the ISM. Fig. 4 shows the temperature versus density for all gas particles in both simulations. The top panel shows simulation L while the bottom panel shows the phase diagram for simulation H. Most particles have a temperature of 10^4 K. In simulation H a large fraction of the particles has a temperature of about 100 K. This simulation shows a dominant two-phase structure, and resembles the ISM in simulations of HSB galaxies (Gerritsen & Icke 1998). Quantitatively, the cold gas fraction ($T < 1000$ K) makes up 37% of the total gas mass in simulation H and only 4% in simulation L. This reflects the cooling properties of the gas: in simulation L seven times less heat input is required to keep the gas at 10^4 K as in simulation H.

Consequently simulation L contains virtually only a warm, one-phase ISM. The simulated absence of metals prevents the ISM from cooling efficiently. As molecular gas is only formed in/from the cold component of the ISM, the 4% mentioned above is actually an upper limit to the amount of molecular gas that could form in such a galaxy. The amount of cold molecular gas in sites for star formation would thus be negligible. From these models we expect the disks of LSB galaxies to contain only negligible amounts of molecular gas. This is consistent with observations by Schombert et al. (1990) and de Blok & van der Hulst (1998b), who find upper limits of less than 10%.

5. Discussion

The structural parameters of the modeled disks appear to be independent from the star formation activity. In this section we

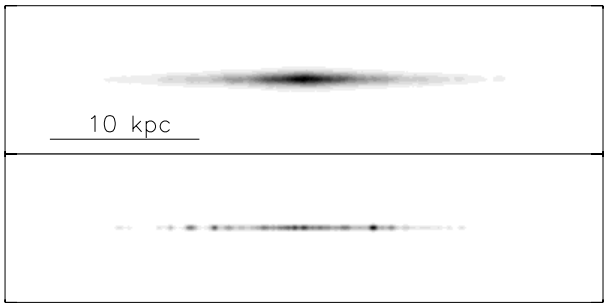

Fig. 5. Edge-on views of the mass and light distribution in LSB galaxy L. The *top panel* shows a linear grey-scale representation of the projected mass surface density. The *bottom panel* shows a grey-scale representation of the projected V-band surface brightness. Here, the star particles formed during the run-time of the simulation are assigned a V-band flux according to their age following Charlot & Bruzual (1993). The contrast has been adjusted to a dynamic range of 5 magnitudes. This view resembles the so-called "chain galaxies" described by Cowie et al. (1995)

will discuss the appearance of the stellar disk of LSB galaxies, and the ISM in LSB galaxies.

5.1. Stellar disk

LSB galaxies are flatter than normal HSB galaxies (cf Fig. 2). From a study of the catalog of edge-on galaxies by Karachentzev et al. (1993), Kudrya et al. (1994) concluded that galaxies become increasingly thinner towards later Hubble types, with the very thinnest galaxies having major over minor axis ratios of 20. Our model galaxies have axial ratios of 15, that is, almost as flat as the flattest galaxies in the Karachentzev et al. catalog. The top panel in Fig. 5 shows the edge-on view of mass distribution in LSB galaxy L.

Our model LSB galaxies support claims made by Dalcanton & Shectman (1996) that some of the extremely flat galaxies ("chain galaxies") detected in medium-redshift HST images (Cowie et al. 1995) are simply edge-on LSB galaxies. Cowie et al. present HST wide-I band observations of these chain galaxies which they describe as "extremely narrow, linear structures... with superposed bright 'knots'." A few of these galaxies were found to lie at a redshift $z \sim 0.5$. As an I-band view of that redshift corresponds approximately to a V-band view locally, we have attempted to simulate a V-band observation of model L edge-on, by assigning to each stellar particle the I-band flux corresponding to its age (Charlot & Bruzual 1993). This is shown in the bottom panel of Fig. 5, where the dynamic range of the picture has been adjusted to correspond approximately with the contrast that the observed chain galaxies have with respect to the sky-background. Comparison with any of the galaxies in Fig. 20 of Cowie et al. will show the resemblance.

How will the edge-on surface brightness distributions of LSB galaxies compare with those of HSB galaxies of similar scale length? Compared to an equally large HSB galaxy, the scale height of an LSB galaxy is smaller. Due to the low dust content in LSB galaxies (McGaugh 1994), effects of edge-brightening will be stronger in the LSB galaxy compared to the dust-rich HSB galaxy. An edge-on LSB might have a higher apparent surface brightness than an edge-on HSB galaxy of the same size. For example, for HSB galaxies in the Ursa Major cluster, Tully et al. (1997) find a differential extinction in the B-band going from face-on to edge-on of 1.8 mag arcsec^{-2}. The LSB galaxies in their sample are found to be almost transparent with a differential extinction of only 0.1 mag arcsec^{-2}. The almost two magnitudes extra extinction in the HSB can thus easily compensate the few magnitudes difference in *intrinsic* surface brightness, making edge-on LSB galaxies as bright in surface brightness as edge-on HSB galaxies.

Hence it is much more difficult to distinguish between edge-on LSB and HSB galaxies than between face-on LSB and HSB galaxies. A smaller number of star forming regions, extreme flatness and blue colors will be the only easily visible distinguishing characteristics.

The reason why the stellar disks of LSB galaxies are so thin is that they are very stable to local instabilities (Fig. 1). As a consequence, bars and spiral structure, which are the most efficient methods for heating a stellar disk (Sellwood & Carlberg 1984), are unlikely to develop spontaneously in LSB galaxies. Thus there is no natural way to make the disks thick.

This explanation is supported by the rarity of barred LSB galaxies. In the LSB galaxy catalog by Impey et al. (1996), only 4 percent of the galaxies are barred, while the frequency of barred galaxies in the RC2 is some 30 percent (Elmegreen et al. 1990). Sellwood & Wilkinson (1993) give a fraction of 2/3 for barred HSB galaxies. The stability of LSB disks is confirmed in a numerical study of the dynamical stability of these systems by Mihos et al. (1997). Whereas we adopted the "most likely" solution for the mass-to-light ratio of stellar disk, these authors considered the "worst case" scenario of maximum disk. However their conclusion is the same as ours: the disks of LSB galaxies are extremely stable.

The lack of truly LSB edge-on galaxies (Schombert et al. 1992) could tell us something about the existence of very LSB galaxies. As shown above, the presently known population of LSB galaxies, when turned edge-on, brightens to surface brightnesses comparable to those of similar-sized HSB galaxies. In principle, the edge-on counterparts of the currently known LSB galaxies should thus already be in the conventional galaxy catalogs, showing up as "streaks on the sky". As truly LSB edge-on galaxies seem to be lacking from the LSB catalogs, this suggests that galaxies with face-on surface brightnesses $\mu_0(B) > 25$ mag arcsec^{-2} are probably very rare.

5.2. Blue and red LSB galaxies

Fluctuations in the SFR as shown in Fig. 3, may very well explain why most of the LSB galaxies detected in surveys are blue. As McGaugh (1996) argues, the selection effects against finding red LSB galaxies on the blue sensitive plates on which surveys have been carried out are quite severe. It will be very hard to find LSB galaxies with colors $B - V \simeq 1$ or redder. So if the absence of red LSB galaxies from the current catalogs is caused

purely by these selection effects, the blue LSB galaxies could simply be the bursting tip of a proverbial iceberg.

In order to explain the colors of the bluest LSB galaxies in the sample of de Blok et al. (1996), van den Hoek et al. (1997) had to invoke bursts with a duration of between 0.5 and 5 Myr and an amplitude between 1 and 5 $M_\odot$/yr. The fluctuations found in our simulation L have an amplitude of 0.15 $M_\odot$/yr, with a duration of about 20 Myr. This duration is determined by the lifetime for OB stars and the collapse time for molecular clouds, which are both of the order of a few 10^7 yr. They are therefore slightly milder than the bursts invoked by van den Hoek et al. (1997), but keep in mind that the latter bursts were used to explain the *bluest* galaxies. Our models attempt to simulate an average LSB galaxy, and it should not come as a surprise that the fluctuations we find are milder. Given the many assumptions and uncertainties in both modeling and observations, it is actually quite encouraging that the parameters agree to within an order of magnitude.

Assuming that blue LSB galaxies are currently undergoing a period of enhanced star formation, implies that there exists a population of *red, non-bursting, quiescent* LSB galaxies. These should then also be metal-poor and gas-rich, and share many of the properties of the galaxies we have been modeling.

We can estimate the fraction of red LSB galaxies by calculating the distribution of the birthrate parameter b for simulation L. The b parameter is the ratio of the present SFR over the average past SFR and is a useful tool for studying the star formation history of galaxies. Birthrate parameters have been determined for a large sample of spiral galaxies by Kennicutt et al. (1994). The trend is that early type galaxies have small values for b, thus most star formation occurred in the past, while late type and irregular galaxies have large values for b, often exceeding 1, indicating that those galaxy are still actively forming stars, and more so than in the past. Here we apply this analysis to simulation L in order to estimate the fractions of blue and red LSB galaxies.

In Fig. 6a we plot the distribution of b values for simulation L (solid line), where we have followed the value of b over the duration of the simulation in steps of 15 Myr. Thus if the SFR peaks in a particular time interval, the corresponding value of b will be high. If the SFR is low in this time interval b is also low. In total we have 200 b values.

Also shown in Fig. 6a are the b distribution for a simulation of an HSB Sc galaxy (Gerritsen & Icke 1998, dotted line) and the mean values for different galaxy types (from Kennicutt et al. 1994). Due to the low average SFR the distribution for the LSB simulation is much broader than the distribution for the HSB simulation, and the average b value is larger.

Also it is clear that the LSB galaxy has b values larger than the average for early type galaxies for most of the time. "Classical" LSB galaxies are blue compared to HSB galaxies, they thus have an excess of recent star formation or equivalently a higher b value. We now define a LSB galaxy to be "blue" if its birthrate parameter b exceeds the average value of b for a HSB late-type galaxy (see Kennicutt et al. 1994 for relations between

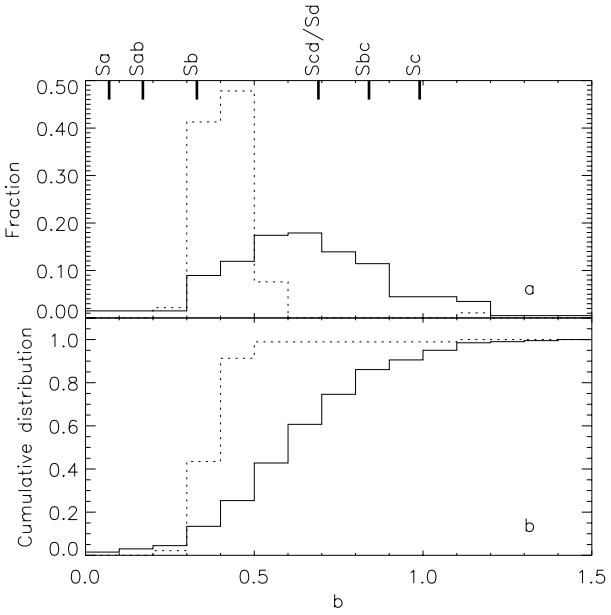

Fig. 6. a Distribution of the birthrate parameter b, the ratio of the current SFR to the average past SFR. Solid line shows the b values derived for simulation L, dotted line shows the b distribution for a simulation of an Sc galaxy (Gerritsen & Icke 1998). On the *top* are average b values for different types of galaxies (Kennicutt et al. 1994). The *bottom panel* shows the cumulative distribution for the two simulations. Less than 20% of the b values for the LSB galaxy are below $b = 0.4$, hence we expect at most 20% of LSB galaxies to be "red"

birthrate parameter and color). Fig. 6a shows that this requires that $b_{LSB} > \langle b_{HSB} \rangle \approx 0.4$.

LSB galaxies that do not meet this requirement are "red": non-bursting, but nevertheless still gas-rich. From Fig. 6b (which shows the cumulative b distribution) we can see that over 80 percent of the fluctuations result in blue LSB galaxies. Less than 20 percent of the fluctuations therefore results in red LSB galaxies.

We can estimate colors of the red population using the burst models from van den Hoek et al. (1997). For example, a 5 Myr burst with an amplitude of 3 $M_\odot$/yr superimposed on a 13 Gyr old population which has undergone an exponentially decreasing SFR with a timescale of 4 Gyr changes colors and surface brightnesses by $\Delta(B-V) \simeq -0.4$, $\Delta(R-I) \simeq -0.2$, $\Delta B \simeq -1$ and $\Delta I \simeq -0.4$ (cf. Table 5 in van den Hoek et al.). Using these values together with the measured colors of the bluest LSB galaxies in de Blok et al. (1995), yields $B-V \sim 1$, $R-I \sim 0.6$ and $\mu_0(B) = 24.5$ for the red population.

A recent CCD survey (O'Neill & Bothun 1997) has picked up a class of LSB galaxies which have $\mu_0(B) \simeq 24$ and $B-V \simeq 0.8$. If some of these galaxies are indeed the non-bursting counterparts of the blue LSB galaxies, they should be metal-poor and gas-rich, and share many of the properties of the galaxies we have been modeling.

In summary, if the blue colors found in LSB galaxies are the result of fluctuations in the star formation rate, then this implies that the red gas-rich LSB galaxies constitute less than 20% of

the gas-rich LSB disk galaxies. This does not rule out the existence of a population of red, gas-poor LSB galaxies. These must however have had an evolutionary history quite different from those discussed here and possibly have consumed or expelled all their gas quite early in their life.

5.3. ISM

The SFRs from both simulations are larger than the observed rate of about $0.05\ M_\odot$/yr. This latter value is probably correct within a factor of 2. Especially the high SFR of simulation H ($0.33\ M_\odot$/yr) is almost an order of magnitude larger than what is needed and it seems impossible to reconcile this value with the observations. Instead the global SFR is consistent with the global SFR for equal-luminosity galaxies (e.g. Kennicutt 1983). For instance the Sc galaxy NGC 6503 with a maximum rotation velocity of $v = 120\,\mathrm{km\,s^{-1}}$ has a total measured SFR of $0.4\ M_\odot$/yr, and a simulated SFR of $0.35\ M_\odot$/yr (Gerritsen & Icke 1997, 1998). In general the SFRs of equal-luminosity galaxies differ by a factor 10 between LSB and HSB galaxy (van den Hoek et al. 1997, and Kennicutt 1983), despite the copious amounts of gas available in the LSB galaxies (de Blok et al. 1996).

SFR_L approaches the correct value and the physical reason is shown in Fig. 4. The essential information to retain from this phase diagram is that we need a different ISM for LSB galaxies, where the bulk of the gas is not directly available for star formation, as it is too warm (of order 10^4 K). The simulations do not include phase transitions from neutral to molecular gas, but as an estimate for the H_2 mass we can consider all star forming gas ($T \lesssim 300$ K) to be molecular. This gas represents less than 2% of the total gas mass. In this respect it is interesting to note that for a small sample of LSB galaxies CO is not detected, yielding an limit of $\mathrm{M(H_2)/M(H\,I)} \ll 30$ percent (de Blok & van der Hulst 1998b, Schombert et al. 1990). A few galaxies have upper limits less than 10%.

As discussed in the previous section the warm ISM may be caused by a low metallicity for the gas. Below 10^4 K, cooling is dominated by heavy elements like C^+, Si^+, Fe^+, O. If these elements are rare then it is difficult for the gas to radiate its energy away.

Direct observational support for a low metallicity ISM in LSB galaxies comes from oxygen abundance measurements of H II regions in LSB galaxies. Those studies yield metallicities of approximately 0.5 times solar metallicity (McGaugh 1994). Measurements of the oxygen abundance in F563-1 (de Blok & van der Hulst 1998a) give an average oxygen abundance of 0.15 $Z_\odot$ (compare with the difference in metallicity between models H and L).

A point of concern is the IMF. Our premise is that the IMF is universal, however it can differ from our adopted Salpeter IMF (see 2.1). Especially a low upper-mass cutoff could easily lead to an underestimation of the SFR (e.g. an upper mass cutoff at 30 $M_\odot$ reduces the measured SFR by 2-3; Kennicutt 1983). However current determinations of the IMF in external galaxies point towards a universal IMF (Kennicutt 1989; Kennicutt et al. 1994). Furthermore, observations suggest that massive stars *are* present in the H II regions of LSB galaxies (McGaugh 1994).

6. Conclusions

What causes the low evolution rate for LSB galaxies? The low density has often been invoked to explain this, since the dynamical time scales with $1/\sqrt{\rho}$. This scenario is exactly what is tested in simulation H. The only difference with a normal HSB galaxy is the scale length of the galaxy, which is for instance three times larger than the scale length for the equally bright galaxy NGC 6503. The result is striking: adopting "standard" values for the star formation process results in a SFR identical to the rates of HSB galaxies.

Thus the low density in itself seems not capable of doing the job, and we have to rely on a scarcity of heavy elements to reproduce a true LSB galaxy. This fits in logically with the notion that stars are the producers of these elements; the low star formation activity prevents metal enrichment of the ISM. It implies that the SFR has been low throughout the evolution of LSB galaxies, and that these galaxies are "trapped" in their current evolutionary state: low density prevents rapid star formation, which prevents enrichment of the ISM, which prevents cooling, resulting in a warm one-phase ISM. So although the lack of metals is directly responsible for the low SFR, the low density may ultimately determine the fate of LSB galaxies.

In summary we reach the following conclusions on the physical properties of LSB galaxies.

1. **Dominant halo:** The dominance of the dark matter halos in LSB galaxies (de Blok & McGaugh 1997) results in very thin and stable disks. The major over minor axis ratios of the stellar disks are larger than 15. Lack of dust in LSB galaxies will result in edge-on LSB galaxies having apparent surface brightnesses equal to those of edge-on HSB galaxies of similar size. The lack of truly LSB edge-on galaxies may indicate that disk galaxies with $\mu_0(B) > 25$ mag arcsec^{-2} are rare.
2. **Low metallicity:** Modeling the low SFR found in LSB galaxies, demands that the metallicity in the ISM must be approximately 0.2 solar, which is consistent with observation by McGaugh (1994) and de Blok & van der Hulst (1998a). These low metallicities prevent effective cooling so that the ISM in LSB galaxies primarily consists of warm ($\sim 10^4$ K) gas. The amount of cold (molecular) gas is probably less than 5% of the H I mass, supporting claims by Schombert et al. (1990) and de Blok & van der Hulst (1998b) who derive small molecular gas fractions.
3. **Low average SFR:** Due to the fluctuations in the SFR in LSB galaxies and their large contrast with the average SFR, the spread in colors among LSB galaxies will be larger than among HSB galaxies. From the distribution of birthrate parameters in our simulations we deduce that, if the currently known blue *gas-rich* LSB galaxies are the most actively star forming LSB galaxies, they constitute over 80 percent of the total population of *gas-rich* field LSB disk galaxies.

This implies that there is at most an additional 20 percent of quiescent, gas-rich LSB disk galaxies. This does not preclude the existence of an additional red, gas-poor population. However this population must have an evolutionary history quite different from that described in this work.

Acknowledgements. We are much indebted to Lars Hernquist for generously providing the TREESPH code. We also thank Frank Briggs and Thijs van der Hulst for their comments on a draft of this paper. We thank the referee, Dr. Friedli, for his extensive comments. The research of JPEG was supported by the Netherlands Foundation for Research in Astronomy (NFRA) with financial aid from the Netherlands Organization for Scientific Research (NWO).

References

Barnes J.E., Hut P., 1986, Nat 324, 466
Bottema R., 1993, A&A 275, 16
Bruzual B.A., Charlot S., 1993, ApJ 405, 538
Charlot S., Bruzual B.A., 1991, ApJ 367, 126
Cowie L.L., Hu E.M., Songaila A., 1995, AJ 110, 1576
Dalcanton J.J., Shectman S.A., 1996, ApJ 465, L9
Dalgarno A., McCray R., 1972, ARA&A 10, 375
de Blok W.J.G., McGaugh S.S., 1996, ApJ 169, L89
de Blok W.J.G., McGaugh S.S., 1997, MNRAS 290, 533
de Blok W.J.G., van der Hulst J. M., 1998a, A&A 335, 412 (Paper I)
de Blok W.J.G., van der Hulst J.M., 1998b, A&A 336, 49 (Paper II)
de Blok W.J.G., van der Hulst J.M., Bothun G.D., 1995, MNRAS 274, 235
de Blok W.J.G., McGaugh S.S., van der Hulst J.M., 1996, MNRAS 283, 18
Dopita M.A., Ryder S.D., 1994, ApJ 430, 163
Elmegreen D.M., Elmegreen B.G., Bellin A.D., 1990, ApJ 364, 415
Field G.B., Goldsmith D.W., Habing H.J., 1969, ApJ 155, L149
Freeman K.C., 1970, ApJ 160, 811
Friedli D., Benz W., 1995, A&A 301, 649
Gerritsen J.P.E., Icke V., 1997, A&A 325, 972
Gerritsen J.P.E., Icke V., 1998, in press
Gingold R.A., Monaghan J.J., 1977, MNRAS 181, 375
Guiderdoni G., Rocca-Volmerange B., 1987, A&A 186, 1
Hernquist L., 1987, ApJS 64, 715
Hernquist L., 1989, Nat 340, 687
Hernquist L., Katz N., 1989, ApJS 70, 419
Impey C.D., Sprayberry D., Irwin M.J., Bothun G.D., 1996, ApJS 105, 209
Karachentzev I.D., Karechentzeva V.E., Parnovsky S.L., 1993, Astron. Nachr. 314, 97
Katz N., 1992, ApJ 391, 502
Katz N., Weinberg D.H., Hernquist L., 1996, ApJ 105, 19
Kennicutt R.C., 1983, ApJ 272, 54
Kennicutt R.C., 1989, ApJ 344, 685
Kennicutt R.C., Tamblyn P., Congdon C.W., 1994, ApJ 435, 22
Kudrya Y.N., Karachentzev J.D., Karachentzeva V.E., Parnovsky S.L., 1994, Astron. Lett. 20, 8
Lamers H.J.G.M.L., Leitherer C., 1993, ApJ 412, 771
Leitherer C., Robert C., Drissen L., 1992, ApJ 401, 596
Lucy L.B., 1977, AJ 82, 1013
McGaugh S.S., 1994, ApJ 426, 135
McGaugh S.S., 1996, MNRAS 280, 337
McGaugh S.S., Bothun G.D., 1994, AJ 107, 530
McGaugh S.S., de Blok W.J.G., 1996, 481, 689
McKee C.F., Ostriker J.P., 1977, ApJ 218, 148
Mihos J.C., Hernquist L., 1994, ApJ 437, 611
Mihos J.C., Hernquist L., 1994, ApJ 431, L9
Mihos J.C., Hernquist L., 1996, ApJ 464, 641
Mihos J.C., McGaugh S.S., de Blok W.J.G., 1997, ApJ 477, 79L
Mo H.J., McGaugh S.S., Bothun G.D., 1994, MNRAS 267, 129
Navarro J.F., White S.D.M., 1993, MNRAS 265, 271
O'Neill K., Bothun G.D., Schombert J., Cornell M.E., Impey C.D., 1997, AJ 114, 2448
Schombert J.S., Bothun G.D., Impey D.D., Mundy L.G., 1990, AJ 100, 1523
Schombert J.S., Bothun G.D., Schnieder S.E., McGaugh S.S., 1992, AJ 103, 1107
Sellwood J.A., Carlberg R.G., 1984, ApJ 282, 61
Sellwood J.A., Wilkinson A., Rep. Prog. Phys. 56, 173
Steinmetz M., 1996, MNRAS 278, 1005
Toomre A., 1964, ApJ 139, 1217
Tully R.B., Verheijen M.A.W., Pierce M.J., Huang J.-S., Wainscoat R.J., 1996, AJ 112, 2471
van Albada T.S., Sancisi R., 1986, Phil. Trans. R. Soc. Lond. A 320, 447
van den Hoek L.B., de Blok W.J.G., van der Hulst J.M., de Jong T., 1997, A&A, submitted
van der Hulst J.M., Skillman E.D., Kennicutt R.C., Bothun G.D., 1987, A&A 117, 63
van der Hulst J.M., Skillman E.D., Smith T.R., et al., 1993, AJ 106, 548
van der Kruit P.C., Searle L., 1982, A&A 110, 61
Wolfire M.G., Hollenbach D., McKee C.F., Tielens A.G.G.M., Bakes E.L.O., 1995, ApJ 443, 152